



Study on the effect of PEG in ionic transport for CMC-NH₄Br-based solid polymer electrolyte

N. K. Zainuddin¹ · N. M. J. Rasali¹ · A. S. Samsudin¹

Received: 15 November 2017 / Revised: 11 February 2018 / Accepted: 19 February 2018 / Published online: 23 March 2018
© Springer-Verlag GmbH Germany, part of Springer Nature 2018

Abstract

The present study investigates the ion transport properties and structural analysis of plasticized solid polymer electrolytes (SPEs) based on carboxymethyl cellulose (CMC)-NH₄Br-PEG. The SPE system was successfully prepared via solution casting and has been characterized by using electrical impedance spectroscopy (EIS), Fourier transform infrared (FTIR) spectroscopy, and x-ray diffraction (XRD) technique. The highest conductivity of the SPE system at ambient temperature (303 K) was found to be 1.12×10^{-4} S/cm for un-plasticized sample and 2.48×10^{-3} S cm⁻¹ when the sample is plasticized with 8 wt% PEG. Based on FTIR analysis, it shows that interaction had occurred at O–H, C=O, and C–O moiety from CMC when PEG content was added. The ionic conductivity tabulation of SPE system was found to be influenced by transport properties and amorphous characteristics as revealed by IR deconvolution method and XRD analysis.

Keywords Biopolymer electrolytes · Amorphous electrolytes · Ion transport properties

Introduction

Over the past century, the utilization of polymers in different applications has outperformed other class of materials that in turn has allowed the polymer industry to grow more rapidly than any other industry in recent years. Polymer electrolyte is an essential component in energy conversion and energy storage system, such as fuel cells, batteries, and dye-sensitized solar [1–3]. Although the performance of such polymer electrolytes is not any better than that of lithium-based electrolytes, they do not pose any safety issues; it has better contact between electrode and electrolytes apart from exhibiting good mechanical properties [4, 5].

Owing to the aforesaid factors, polymer electrolytes have received due attention from researchers, particularly of those who aim of utilizing the polymer electrolytes as polymer host based on natural polymers in proton conducting of solid polymer electrolytes (SPEs). Different types of natural polymers have been investigated, namely, rice starch [6], chitosan [7],

iota-carrageenan [8], and methylcellulose (MC) [9]. Previous works have demonstrated that natural polymer possesses the ability to solvate the dopant that supplies mobile ions, in the event that there is a direct interaction between the lone pair electron of the heteroatom, i.e., oxygen or nitrogen in the polymer [10, 11]. A potential candidate to act as polymer host for solid electrolyte is carboxymethylcellulose (CMC). CMC is one of the cellulose derivatives which displays biodegradable and non-hazardous properties [12]. It has been widely used in different industrial applications such as in the food industry as a thickener and a binder, in the oil industry as a lubricant for oil production, and in the cosmetic industry as a stabilizer [13]. In this work, CMC is chosen as it has good film-forming property, high mechanical intensity, and ability to form transparent film [14].

Several approaches were suggested in the literature in order to enhance the conductivity performance, including the use of blend polymers, the addition of a ceramic filler, plasticizer, and even radiation [15]. According to Bhide et al. [16], the addition of plasticizer is the simplest and most effective way to improve the conductivity of SPEs in comparison to other techniques. Examples of plasticizer which has been employed in polymer electrolytes systems include ethylene carbonate [17], glycerol [18], dimethylacetamide (DMA) [19], and tetra (ethylene glycol) dimethyl ether [20] among others. These plasticizers were chosen based on a number of properties such as

✉ A. S. Samsudin
ahmadsalihin@ump.edu.my

¹ Advanced Materials Group, Faculty of Industrial Sciences & Technology, Universiti Malaysia Pahang, Gambang, 26300 Kuantan, Pahang, Malaysia

high dielectric constant, its ability to enhance the ionic dissociation, low viscosity, decrease the glass transition, and increase the amorphous content [21–23].

In the present work, a proton-conducting SPE system based on CMC-NH₄Br plasticized with PEG was prepared and investigated. The CMC-NH₄Br-PEG-based SPE system have been characterized via Fourier transform infrared (FTIR) spectroscopy, electrical impedance spectroscopy (EIS), and x-ray diffraction (XRD) in order to study the interaction between polymer-salt complexes plasticized with PEG by determining the functional group that introduces in the complexation SPEs, the degree of crystallinity to establishes the amorphousness nature of SPEs, and the electrolyte composition that yields the best electrical conductivity. Moreover, for further investigation in ionic transport properties of SPEs, the FTIR vibrational effect was evaluated by using deconvolution method to confirm the conduction of ions that dissociate in the SPEs electrolyte system.

Experimental

Preparation of solid polymer electrolytes

In this present work, SPE system has been prepared via solution cast technique; 25 wt% NH₄Br (Merck Co.) was added into CMC (Acros Organics Co.) solution, and the mixture was stirred continuously until complete dissolution was obtained [24–26]. Then, the various compositions of PEG ($M_w \sim 1100$: Sigma Aldrich Co.) plasticizers were added (in wt%) into the mixture and were stirred until it becomes a homogenous solution. The homogeneous solution was then casted into several Petri dishes and left dried at room temperature until film form. For further drying, the dried sample was put it in the desiccators before being characterized to ensure that no water content or gelling form obtained in the polymer electrolyte system. The compositions of PEG and classification of the sample for SPEs system are tabulated in Table 1.

Table 1 List of samples with their compositions respectively

Samples	CMC (g)	NH ₄ Br (g)	PEG (wt%)
A			0
B			2
C			4
D	2	0.6666	6
E			8
F			10
G			12

Characterization of CMC-NH₄Br SPEs system

EIS

The ionic conductivity of SPEs system was analyzed via EIS using HIOKI 3532-50 LCR Hi-Tester at a different frequency in the range of 50 Hz to 1 MHz. The sample was cut into a suitable size and placed between two stainless steel blocking electrodes of the sample holder. The ionic conductivity of SPEs system was calculated using the equation:

$$\sigma = \frac{d}{R_b A} \quad (1)$$

where d is the thickness of the sample, R_b is the bulk resistance, and A is the cross-sectional area.

FTIR spectroscopy

FTIR spectroscopy measurement was carried out using PerkinElmer Spectrum in order to confirm the complexation in the SPEs system. The spectrometer was equipped with an attenuated total reflection (ATR) accessory. The germanium crystal was used for ATR, and the infrared light was passed through the sample in the range of 700–4000 cm⁻¹ with a resolution of 4 cm⁻¹.

Deconvolution study

The FTIR deconvolution was carried out using Gaussian-Lorentz function adapted to the Origin Lab 9.0 software. In the deconvolution method, the FTIR peaks due to the dominant ionic movement were selected, and the sum of the intensity of all the deconvoluted peaks was ensured to fit the original spectrum. The area under the peaks was determined, and the free ions (%) were calculated using the equation [27, 28]:

$$\text{Free ions (\%)} = \frac{A_f}{A_f + A_c} \times 100\% \quad (2)$$

where A_f is an area under the peak representing the free ions region, A_c is the total area under the peak representing the contact ions, M is the moles of each wt% PEG, N_A is the Avogadro's constant, V_{total} is the total volume of SPEs system, k is the Boltzmann constant, T is the absolute temperature, and e is electron charge. The number density (η), mobility (μ) and diffusion coefficient (D) of the ions were calculated with the following equation [29–31]:

$$\eta = \frac{MN_A}{V_{\text{Total}}} \times \text{free ions (\%)} \quad (3)$$

where

$$V_{Total} = \left[\frac{weight}{density} (CMC + NH_4Br) \right] + \left[\frac{weight}{density} (PEG) \right] \quad (4)$$

$$\mu = \frac{\sigma}{\eta e} \quad (5)$$

$$D = \frac{kT\mu}{e} \quad (6)$$

XRD

XRD-Rigaku MiniFlex II was employed to study the nature of samples whether amorphous or crystalline or both [32]. It was directly scanned at angle 2θ between 5° and 80° with 1.5406 Å wavelength generated by a CuKα source. In XRD deconvolution technique, Origin Lab 9.0 software was used, and the baseline function was applied to the specified region. By using the Gaussian function, the amorphous and crystalline peaks were deconvoluted, and all peaks were ensured to fit the original spectrum. After extracting the peak, the area under the peaks was determined, and the percentage of crystallinity was calculated using Eq. (7) below [33, 34].

$$X_c = \frac{A_c}{A_T} \times 100\% \quad (7)$$

where A_c is an area of the crystalline region; A_T is the total area under the peak representing the area of the crystalline region, A_c , and area of the amorphous region, A_a ; and X_c is the degree of crystalline in percentage.

Result and discussion

Impedance analysis

MacDonald [35] reported that the impedance spectroscopy (EIS) gives a good overview, especially to solid-state phenomena. It should be understood as “immittance,” i.e., any form of the transfer function of two terminal systems: impedance Z , admittance $Y = Z^{-1}$; modulus $M = j\omega C_o Z$; and complex permittivity M^{-1} , where $j = \sqrt{-1}$, ω is angular frequency ($\omega = 2\pi f$), and C_o is the permittivity of free space. The principle of its operation is relatively straightforward: a series of small-amplitude ac signals spanning a broad frequency range is applied to a multiphase system. Analysis of the ensuing electrical response via electrical circuit theory results in a complete description of the physicochemical properties of the system. Figure 1 shows the Cole-Cole plots at ambient temperature (303 K) for various sample of SPEs system.

Based on Fig. 1, it can be observed the Cole-Cole plots only consists of a spike line which can be related to the

migration of ions which may occur through the free volume of the matrix polymer and this can be represented by a resistivity element of the present sample [36]. Moreover, the spike line is attributed to the influence of electrode polarization, which is the characteristic of the diffusion process and it also indicates that the current carriers are ions and the total conductivity is mainly the result of ion conduction of SPEs system [37–39]. The inclination of the spike in Cole-Cole plot as observed in the present system shows an angle less than 90° with the real axis when PEG was added and this is attributed to the non-homogeneity or roughness of the electrode-biopolymer electrolytes interface [40].

Since the spike in this present system did not arise at the origin with the addition of PEG for SPEs system, the equivalent circuit is implied to consist of a resistor and constant phase element (CPE) in series connection. CPE can be assumed as a leaky capacitor, to compensate for non-homogeneity between electrode-SPE surface [40]. As shown in Fig. 1, the impedance of the expected equivalent circuit fits the experimental impedance data very well. The value Z_r and Z_i associated to the equivalent circuit can be expressed as [41, 42]:

$$Z_r = R_b + \frac{\cos\left(\frac{\pi p}{2}\right)}{C\omega^p} \quad (8)$$

$$Z_i = R_b + \frac{\cos\left(\frac{\pi p}{2}\right)}{C\omega^p} \quad (9)$$

where

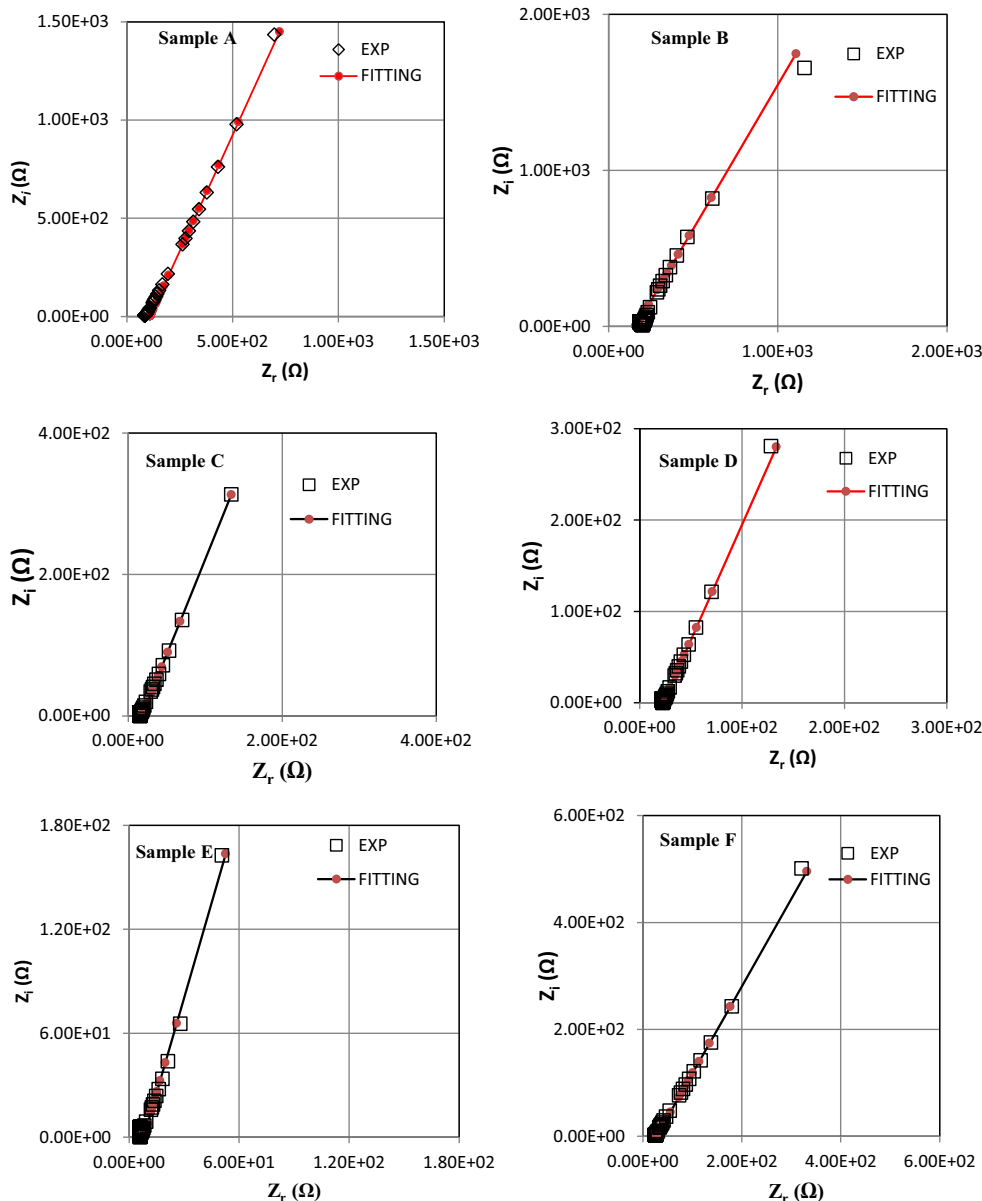
$$Z_{(total)} = Z_r - jZ_i \quad (10)$$

where C is the capacitance of CPE, ω is the angular frequency ($\omega = 1/f$; f is frequency in Hz), p is related to the deviation of the plot from the axis, and j is $\sqrt{-1}$ and the real and imaginary parts of impedance, Z_r and Z_i , respectively.

Based on theoretical fitting in Fig. 1, the parameter of the circuit elements for SPEs system is tabulated in Table 2. Shuhaimi et al. [43] report that if $p = 1$, $Z_{total} = R - j/\omega C$; if $p = 0$, the constant phase element is a perfect resistor where Z_{total} is frequency independent and if the value of p lies between 0 and 1, CPE will act in a way intermediate between a resistor and a capacitor for conducting sample. From Table 2, it shows the value of p lies between 0 and 1, and this reveals that the SPEs system has a resistive and capacitive behavior which is similar as reported in [43].

It is evident that the sample becomes more capacitive than resistive as the PEG composition increases. The bulk resistance, which was obtained from the intercept of the Cole-Cole plot with the Z_r axis decreases as the PEG is increased. The increase in capacitance values with

Fig. 1 The Cole-Cole plot of various samples SPEs system



increasing plasticizer is in good agreement with the following equation [44, 45]:

$$C = \frac{\epsilon_0 \epsilon_{TA}}{d} \tag{11}$$

where ϵ_0 is vacuum permittivity and ϵ_r is dielectric constant.

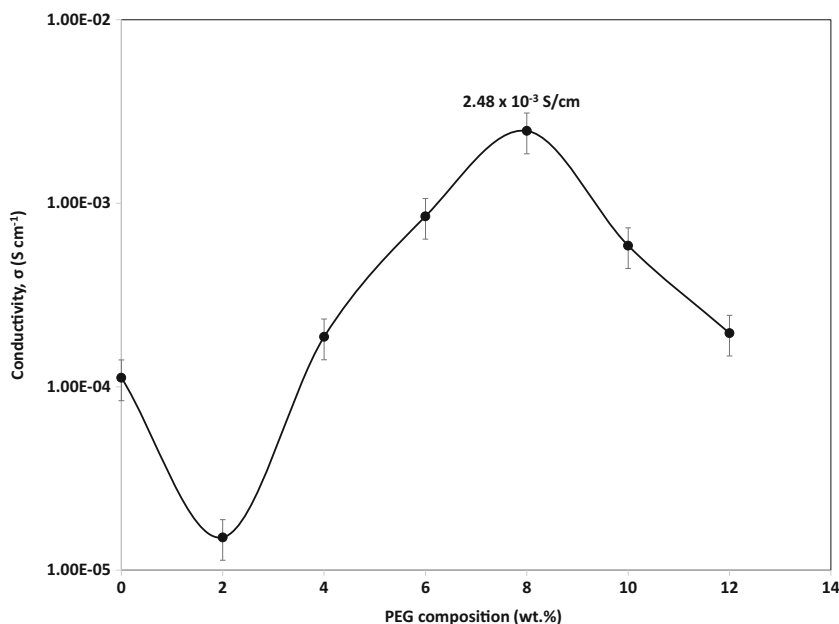
Ionic conductivity analysis

The effect of PEG composition on the conductivity at room temperature is depicted in Fig. 2. Based on [46], the highest conductivity for un-plasticized SPEs system containing with CMC-NH₄Br is achieved at 1.12×10^{-4} S cm⁻¹ for the sample with 25 wt% NH₄Br. For the present system, the addition of PEG is found to influence the increment in ionic conductivity except for sample B which contains 2 wt% of PEG. The decrease of ionic conductivity at lower PEG composition may be due to the insufficient energy from PEG for ions (H⁺) to detach from NH₄⁺ substructure of NH₄Br in order to migrate into

Table 2 The value of circuit elements of the SPEs system

Samples	C (F)	p (radian)	R _b (Ω)
A	9.68×10^{-6}	0.71	109
B	3.14×10^{-6}	0.68	201
C	3.83×10^{-5}	0.71	22.8
D	4.04×10^{-5}	0.72	18.0
E	7.03×10^{-5}	0.80	1.11
F	4.95×10^{-5}	0.81	7.98
G	4.12×10^{-5}	0.73	28.1

Fig. 2 The ionic conductivity at room temperature for SPEs system



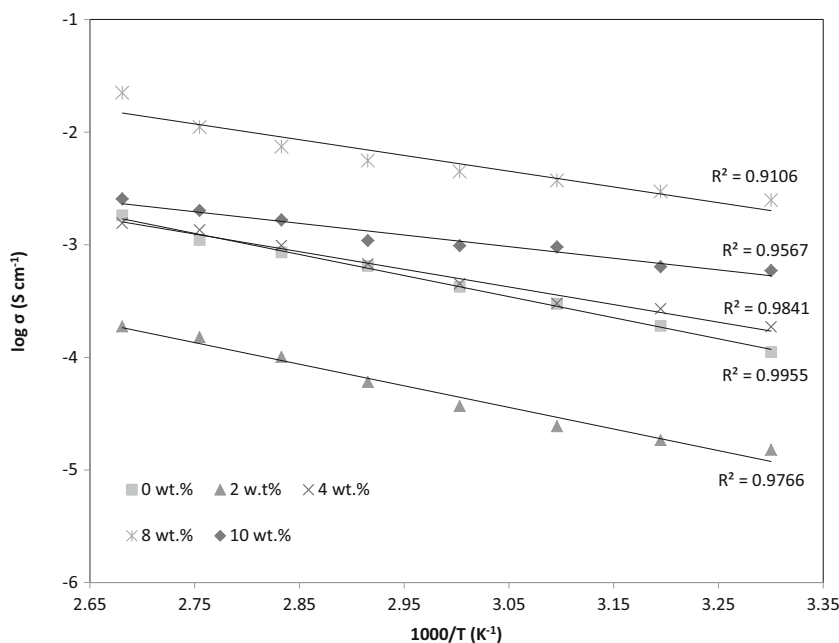
COO⁻ group of CMC. The addition of PEG at lower composition could cause the delaying of ions pathway to migrate towards polymer backbone thus the reduction in ionic conductivity was observed. Furthermore, the small amount of PEG suggests that the PEG is not able to overcome the rate of ion association between CMC and NH₄Br, thus demonstrating a decrease in conductivity [47].

The highest ionic conductivity for the present system is achieved at $2.48 \times 10^{-3}\ S\ cm^{-1}$ for sample containing 8 wt% PEG. This observation suggests that the amount plasticizer is sufficient to assist the dissociation of H⁺ for undissociated H⁺ of NH₄Br, allowing the released of H⁺ for migration towards

COO⁻ group of CMC. As a result, an increase in the ionic conductivity and transport properties in SPEs system are observed [48–50]. The decrease in crystalline content or an increase in amorphous content is expected to influence an increase in conductivity [51] of these SPEs system, and these observations can be proven from XRD analysis which will be discussed later.

Apparently, it shows that beyond 8 wt% of CMC-NH₄Br-PEG SPE system, the conductivity starts to decrease and it may be due to the re-association of the ions [52]. In the present system, the PEG does not supply ions towards CMC-NH₄Br, but it is believed that PEG assisted in dissociating more dopant

Fig. 3 Temperature dependence of ionic conductivity for CMC-NH₄Br-PEG SPE system



into ions, hence, increasing the ionic conductivity and transports mobility [53].

Figure 3 shows the temperature dependence of ionic conductivity for CMC-NH₄Br-PEG system investigated in the temperature range from 303 to 373 K in order to understand the conductivity-temperature behavior of SPE salt polymer system plasticized with the PEG films. It can be observed that the conductivity increase gradually with the increase in temperature, which shows that the SPE system is thermally assisted. The regression values, R^2 was close to unity [39, 40, 54], which indicates that the temperature-dependent ionic conductivity revealed that the SPEs system obeys the Arrhenius rule via the following equation:

$$\sigma = \sigma_0 \exp\left(\frac{-E_a}{kT}\right) \quad (12)$$

where σ_0 is the pre-exponential factor, E_a is the activation energy, and k is the Boltzman constant.

FTIR analysis

Figure 4 shows the possible interaction between the CMC-NH₄Br-PEG for SPE system in the region wave number between 3600 and 900 cm^{-1} . Researchers [55–57] reported that from the FTIR spectra, polymer electrolyte structure according to their

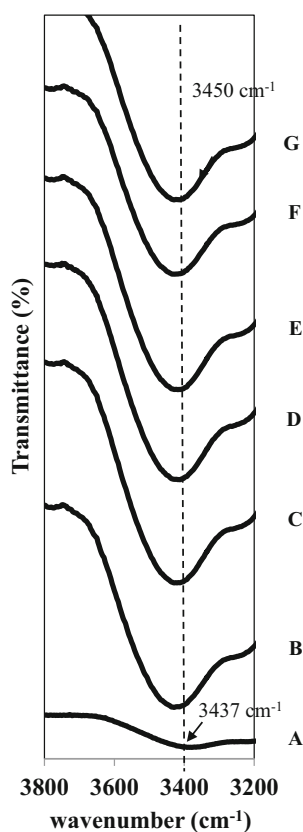


Fig. 4 FTIR spectra of CMC-NH₄Br-PEG SPEs system from 3200 to 3700 cm^{-1}

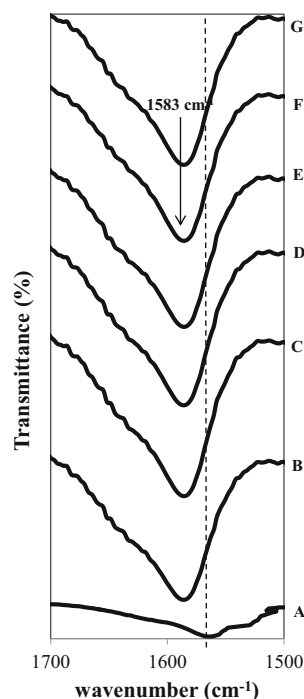


Fig. 5 FTIR spectra of CMC-NH₄Br-PEG SPEs system from 1500 to 1700 cm^{-1}

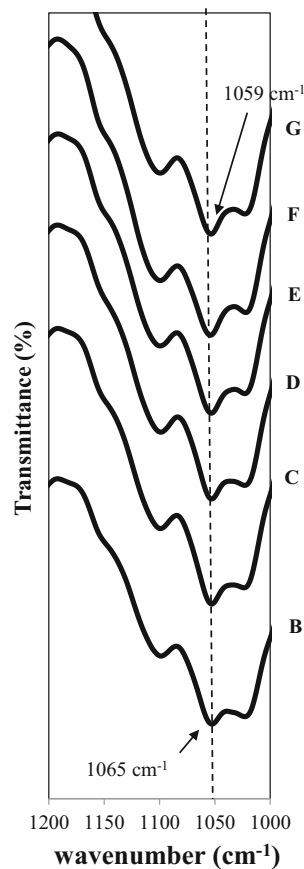


Fig. 6 FTIR spectra of CMC-NH₄Br-PEG SPEs system from 1000 to 1200 cm^{-1}

compositions and the occurrence of complexation and interactions between CMC, NH_4Br , and plasticizer (PEG) could be investigated. Based on the previous work done by Samsudin et al. [46], the main component of polysaccharide CMC can be found at wave number 3236 cm^{-1} shifted to 2920 cm^{-1} , 1589 cm^{-1} shifted to 1587 cm^{-1} , and 1066 cm^{-1} shifted to the 1050 cm^{-1} that attribute to O–H bending, C=O stretching, and C–O⁻ of carboxylate anions of CMC [58–60] and these peaks were identified an interaction when NH_4Br was added.

Based on Fig. 4, it can be clearly seen that the slight different broadness of the peak at 3450 cm^{-1} corresponds to the hydroxyl group (O–H) of plasticizer composition and this band are also comparable with the result observed by Yu et al. [61]. The peak begins to decrease in the broadness in the region of range 3437 to 3450 cm^{-1} when the PEG is increased to up to 12 wt%. Hydrogen bonding of alcohols to electronegative atoms or ions reduces the frequency and broadens the FTIR band associated with the O–H stretch. Samsudin et al. reported that the hydrogen

bonding of the monomeric (O–H) shifts from a sharp band to broadband with the addition of ammonium salt to the solution [62]. The shifts in (O–H) indicates that the intra and intermolecular hydrogen bonding between PEG and various anions are complicated. This observation is evident, as the addition of plasticizers caused the peak intensity of the samples to increase and the growth in the number of free ions, which in turn, influence the change of ionic conductivity [63].

Figure 5 shows the FTIR spectrum of CMC- NH_4Br -PEG in the region from 1500 to 1700 cm^{-1} . Based on Fig. 5, an absorption peak appeared at 1583 cm^{-1} corresponding to the C=O stretching moiety of CMC. The intensity of the peak at 1583 cm^{-1} is clearly found to increase as the content of PEG is increased to up to 8 wt% as shown in Fig. 5. This implies that PEG can serve as an alternative transit site for ion conduction for H^+ from NH_4Br towards C=O of the carboxyl group in CMC for SPEs system. It is believed that the use of PEG allows for the dissociation of more H^+ from NH_4Br and it

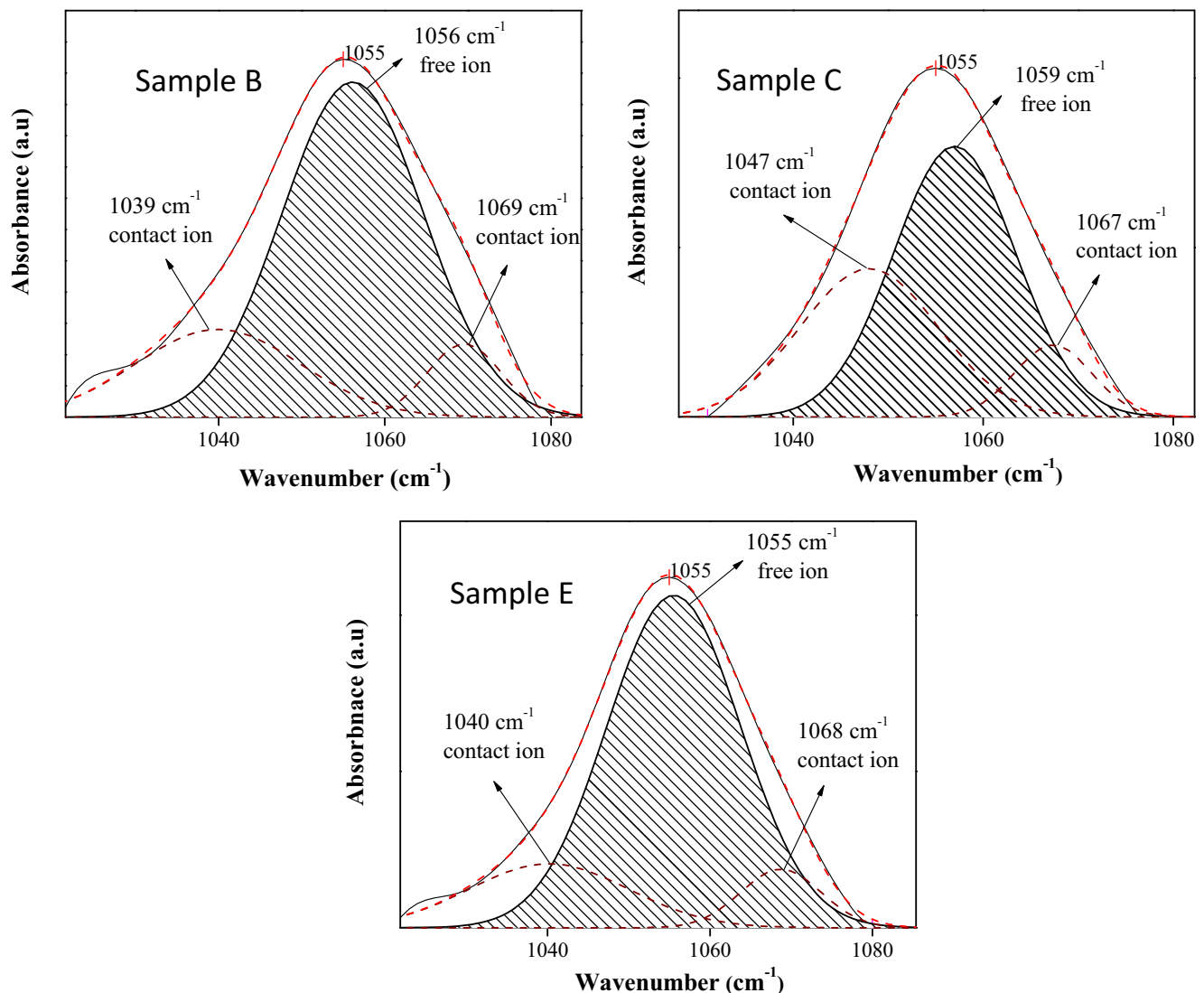


Fig. 7 The deconvolution IR spectrum for various sample of SPEs system

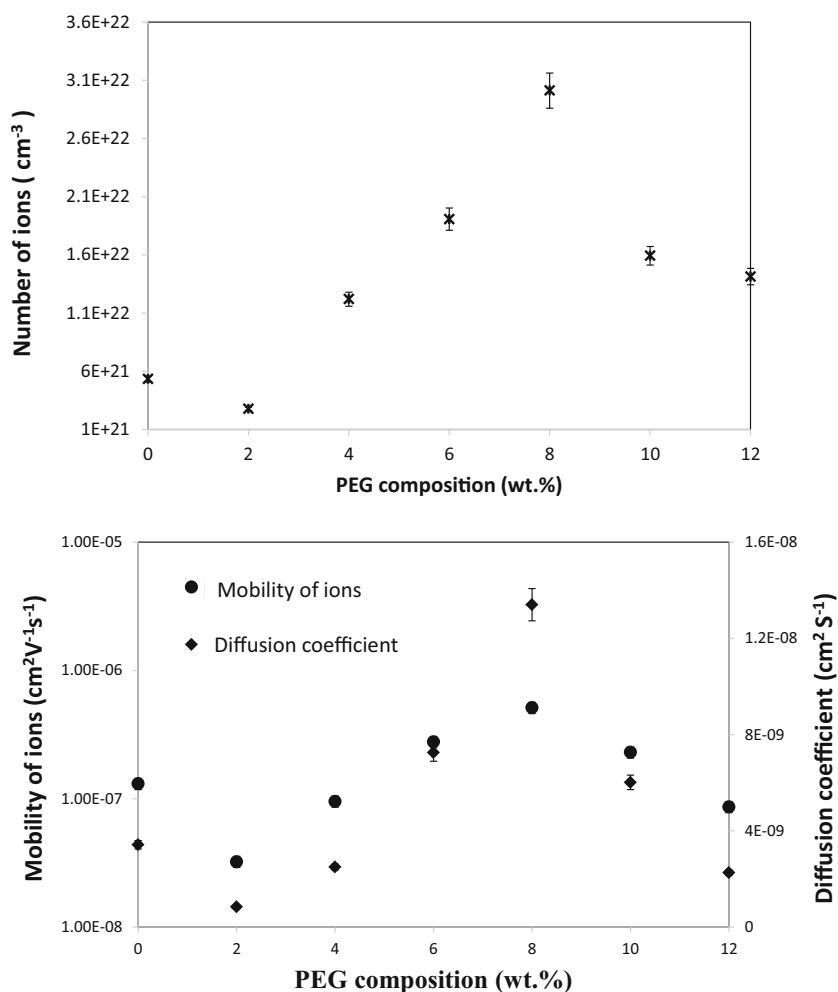
Table 3 The free and contact ions of the CMC-NH₄Br-PEG SPEs system

Samples	Free ions (%)	Contact ions (%)
A	8.637	91.363
B	24.246	75.754
C	55.875	44.125
D	60.852	39.148
E	74.908	25.092
F	32.861	67.139
G	25.241	74.759

would create a shorter distance or new pathway for ion migration in order to interact with C=O. This observation is similar to the observation of Nirali et al. [64], where the interaction occurred when plasticizer was added in the polymer-salt complexes, consequently influencing either the intensity of peak

or changes of wave number in FTIR spectra. On the other hand, it can be seen that the intensity of the peak at 1583 cm⁻¹ begins to decrease when PEG is added beyond 8 wt%, and this is expected due to the overcrowding of H⁺ ions in CMC-NH₄Br-PEG SPEs system where it is expected that the ions start recombined to form neutral ion aggregate as NH₄Br.

Meanwhile, in Fig. 6, peaks at 1065 cm⁻¹ corresponds to C–O⁻ moiety of carboxylate anion from COO⁻ was found to decrease to a lower wave number at 1059 cm⁻¹ when PEG was added. A more significant band in comparison to C=O from CMC where the interaction has occurred in this band. The shifted peak shows the more H⁺ interacted at C–O⁻ of CMC and this may be due to the strong absorbance band which similarly observed by Chai et al. [65] and Kamarudin et al. [66]. Based on the observation, it is proved that the addition of PEG in CMC-NH₄Br SPEs system has performed as an agent in enhancing the dissociation of NH₄Br towards CMC.

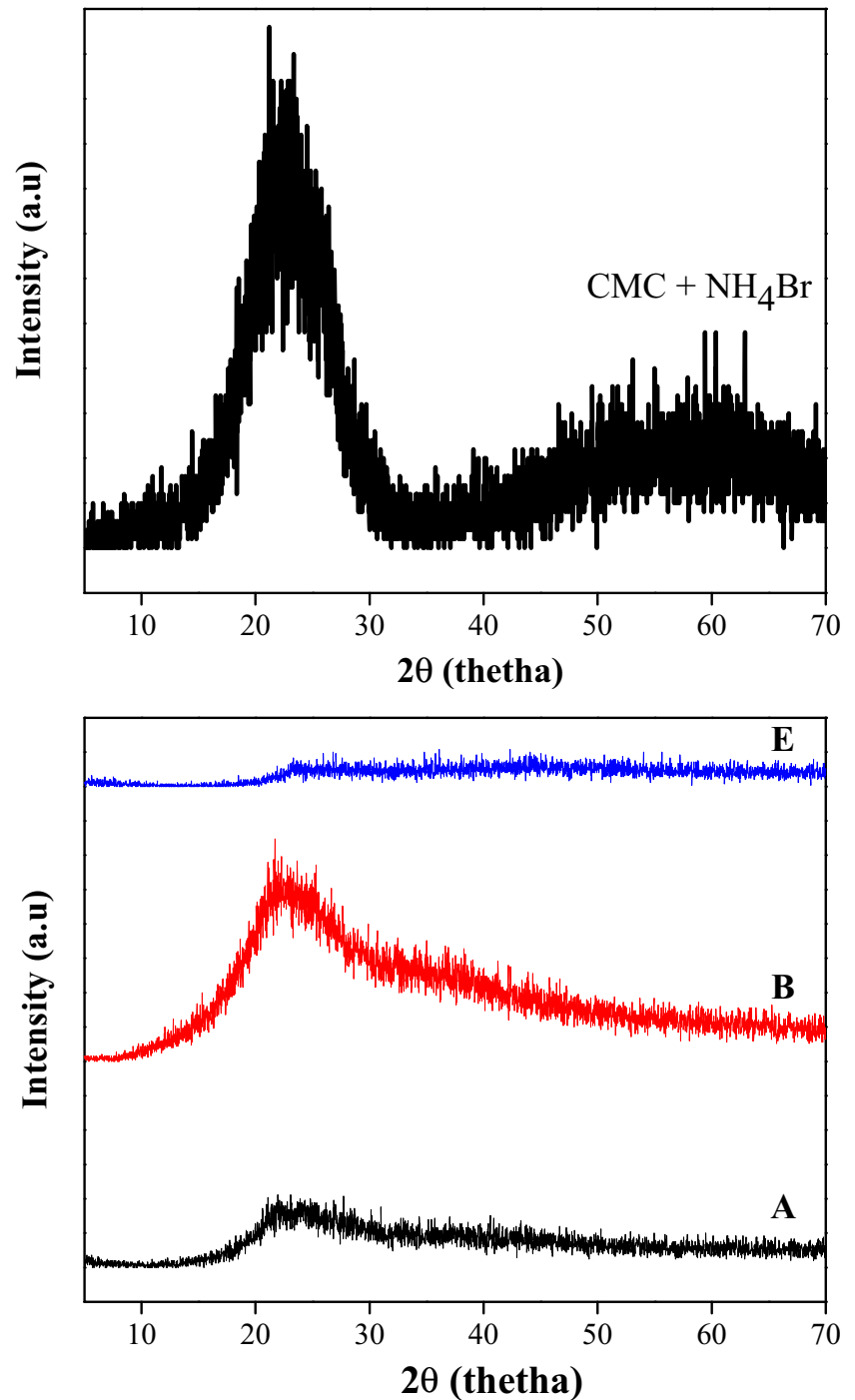
Fig. 8 The transport properties for CMC- NH₄Br-PEG SPEs system

Deconvolution analysis

In the present work, wave numbers between 1040 and 1080 cm^{-1} were used for deconvolution analysis where it is believed the complexes between CMC- NH_4Br and PEG has occurred as proven from FTIR analysis. Figure 7 presents the deconvolution spectra for various sample of CMC- NH_4Br -PEG SPEs system.

Based on Fig. 7, the peak at $\sim 1055 \text{ cm}^{-1}$ that attributed to free anions, conversely, the peaks at $\sim 1040 \text{ cm}^{-1}$ represents the contact ion pairs, and 1068 cm^{-1} is an indication for the formation of ion aggregates [67, 68]. The percentage area of free ions and contact ions were calculated from the ratio of the area of free or contact ions to the total area of deconvolution peaks, respectively. Table 3 shows the percentage of free ions and contact

Fig. 9 XRD spectra for various sample of SPEs system at ambient temperature



ions of the CMC-NH₄Br-PEG SPEs system. Based on Table 3, it can be seen that the percentage of free ions increased when PEG content is added until 8 wt%. The increase of the ion dissociation corresponds to the free ions from the plasticizer, and the H⁺ ions of the NH₄⁺ from the salt improve the ionic conductivity as observed from ionic conductivity analysis. The percentage of free is inversely proportional to the percentage of contact ions. The decrease of free ions at 10 to 12 wt% relates to the formation of ion pairing/aggregate consequently reduced the rate of increment in ionic conductivity.

From the free and contact ions in Table 3, the number of mobile ions (η), ionic mobility (μ), and diffusion coefficient (D) can be calculated using the equation as presented in Eqs. (3), (5), and (6). Figure 8 depicts the transport parameter of CMC-NH₄Br-PEG SPE system.

Based on the literature, the ionic conductivity of a polymer is generally linked to the number of ions and the mobility of conducting species in the polymer complexes [69–71] with the relation base Eq. (5).

From the transport properties, as shown in Fig. 8, it can be inferred that the conductivity is governed by the number of mobile ions, ionic mobility and diffusion coefficient. The increase of η value from 4 to 8 wt% of PEG composition were observed and this attributed to the enhancement of dissociation of H⁺ from NH₄Br when the PEG was introduced in the present system. This result obtained is in reasonable agreement with the changes of FTIR analysis where the interaction influenced to the contribution of ion transport characteristic. Moreover, it also related to the increase in the facilitation of the H⁺ coordination in the plasticized system, enabling continuous motion of charge carrier that led to the maximum ionic conductivity of CMC-NH₄Br-PEG SPE system. With the increment of the dissociation of H⁺, the conductivity for SPE system does respond better from the association of ion count and this is demonstrated through the increase of μ and D that corresponds to the conductivity until it reaches the optimum composition [72, 73]. This is due to the flexibility of the segmental motion of the polymer chains in the SPEs system which leads to the enhancement of the transport properties and conductivity [74, 75].

On the other hand, it shows that the transport properties of SPEs system were found to decrease at higher PEG composition (> 8 wt%). This is primarily due to the aggregation of the ions, which leads to the formation of ion cluster where the dipole interaction between the H⁺ in the medium increases. This, in turn, reduces the charge carriers and thus the conductivity [73]. The value of η , μ , and D calculated is in reasonable agreement with that obtained in refs. [46, 63, 76]. Therefore, it is proven that Eq. (5) fits well in the present work.

XRD analysis

Figure 9 shows the XRD pattern of un-plasticized and plasticized samples of CMC-NH₄Br-PEG complexes. It can be found that the diffraction peak became less intense and more broad due to disruption of amorphous phase when PEG was added in the present system. These results are in agreement with the findings of Itoh et al. [77] and Rajendran et al. [78], where it was found that the plasticizer, which is inserted in polymer electrolytes system, would reduce the non-conductive crystalline phase to obtain better ionic conductivity. A similar observation is found by Leo et al. [79] where further dilution of the crystalline phase can be noticed with the addition of the plasticizer as the sharp peaks in the XRD pattern becomes broadened and less intense.

The hump peak observed between $2\theta = 20^\circ$ and 30° for SPEs system broadened and shifted to the higher angle as the amount of the plasticizer is increased. The pattern shows that the amorphousness of biopolymer electrolytes increases with the increase of the PEG composition. The increase in the broadness of the peak reveals the amorphous nature with some localized ordering of the complexed system is observed in the present system [63, 80]. Hence, it would lead to an increment of the ionic conductivity in the SPEs as observed from the conductivity analysis. The results are in accordance to the findings of Majid and Arof [55] where they observed that the conductivity of the polymer electrolytes is believed to be affected if there is a change in amorphousness of polymer electrolytes system.

Figure 10 demonstrates the XRD deconvolution pattern of various samples for SPEs system. Based on the deconvoluted XRD pattern, the intensity of crystalline peaks decreases and the peak width broadens due to the breaking of order or folding patterns of polymer chain which enhances the amorphousness of the SPEs sample. This implies that the crystallinity of the SPEs is hindered by the addition of PEG, resulting in a more flexible SPEs and thus improves their ionic conductivity [81].

Table 4 shows the percentage of crystallinity (X_c) of CMC-NH₄Br-PEG SPEs system decreases with the addition of plasticizer except for sample B. The increase of crystallinity (X_c) in sample B is attributed due to the amount of residual crystallinity given by the PEG which was found to decrease the ionic conductivity [26, 82]. Moreover, this observation may also be due to the ion trapped in CMC-NH₄Br SPEs system when 2 wt% of PEG was added. This can be demonstrated from the transport properties analysis where the number of ions (H⁺) suddenly decreases which reflected in the reduction of the mobility and diffusion coefficient of ions. In the present system, sample E represents the lowest value of X_c , and this suggests that the addition of the PEG has affected the amorphous nature of the SPEs system. As stated by Rahaman et al. [83], the percentage of crystallinity is inversely proportional to the amorphousness of the SPEs, which means that the

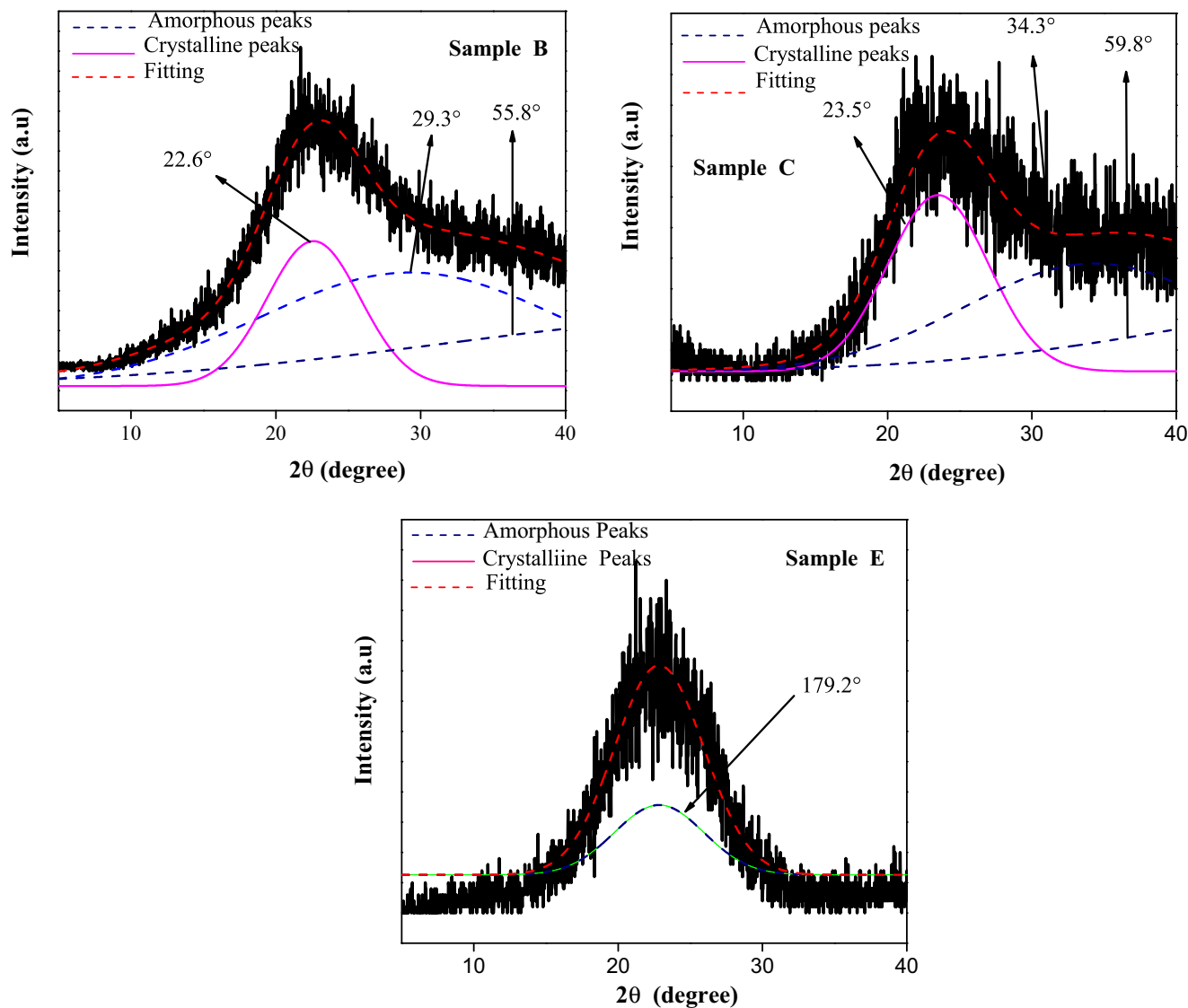


Fig. 10 XRD deconvolution for various samples of SPEs system

decreased of X_c indicates the increase of the amorphous of the SPEs. As reported by Zhou et al. [84], the decrease of crystallinity is probably associated with the progressively higher chain mobility that is facilitated by the corresponding plasticizer which eliminates the cohesive forces between CMC or NH_4Br molecules that in turn enhances the chain mobility, resulting in a lower percentage of crystallinity, X_c .

Table 4 XRD deconvolution parameter for various samples of CMC- NH_4Br -PEG SPE system

Samples	Crystallinity phase	Amorphous phase	X_c (%)
A	8382.89	19,082.69	30.52
B	89.62	179.24	33.33
C	253.04	960.76	20.85
E	585.23	3602.26	13.98

Conclusion

The conducting SPEs based on CMC doped with ammonium bromide (NH_4Br) plasticized PEG was investigated with different composition of PEG by solution casting method. The highest room-temperature ionic conductivity for the SPEs system is observed at $2.48 \times 10^{-3} \text{ S cm}^{-1}$ with a composition of 8 wt% PEG at room temperature. According to the FTIR results, there is a strong contribution of hydrogen bonding of polymer-salt binary system that influences the coordination interaction of H^+ to the to the C=O stretching moiety of CMC, as well as the hydroxyl band, that shifts to higher wave numbers with the increase of the PEG content. From the deconvolution method, the number of ions, mobility of ions, and diffusion coefficient properties demonstrated that the free ions dominated in the ionic transport of SPEs system attribute to the result of the ionic conductivity. The addition of PEG

plasticizer to up to 10 wt% into CMC-NH₄Br SPEs has increased the amorphousness of the electrolyte sample. This has been proven by calculation of the degree of crystallinity of CMC-NH₄Br-PEG-electrolyte system from the XRD analysis via deconvolution. From the results obtained, it is apparent that the present solid polymer electrolytes based carboxymethyl cellulose-NH₄Br plasticized with PEG has the potential to be used for electrochemical applications.

Funding The authors would like to thank MOHE for FRGS grant (RDU170115) and UMP internal grant (RDU 1703189 and PGRS 170308), Faculty Industrial Science and Technology, Universiti Malaysia Pahang for the technical and research support.

References

- Fenton DE, Parker JM, Wright PV (1973) Complexes of alkali metal ions with poly(ethylene oxide). *Polymer* 14:589–594
- Liang YH, Wang CC, Chen CY (2008) Synthesis and characterization of a new network polymer electrolyte containing polyether in the main chains and side chains. *Eur Polym J* 44:2376–2384
- Wright PV (1975) Electrical conductivity in ionic complexes of poly(ethylene oxide). *Br Polym J* 7:319–327
- Armand MB, Chabagno JM, Duclot MJ (1978) Poly-ethers as solid electrolytes. In Proceedings of the second international meeting on solid electrolytes, St. Andrews Scotland. 20–22
- Shukur MF, Kadir MFZ (2015) Hydrogen ion conducting starch-chitosan based electrolyte for application in electrochemical devices. *Electrochim Acta* 158:152–165
- Khanmirzaei MH, Ramesh S (2014) Studies on biodegradable polymer electrolyte rice starch (RS) complexed with lithium oxide. *Ionics* 20:691–695
- Majid SR, Idris NH, Hassan MF, Winnie T, Khiar ASA, Arof AK (2005) Transport studies on filler-doped chitosan based polymer electrolyte. *Ionics* 11:451–455
- Jumaah FN, Mobarak NN, Ahmad A, Ghani MA, Rahman MYA (2015) Derivative of iota-carrageenan as solid polymer electrolyte. *Ionics* 21:1311–1320
- Abdullah OG, Aziz SB, Rasheed MA (2018) Incorporation of NH₄NO₃ into MC-PVA blend-based polymer to prepare proton-conducting polymer electrolyte films. *Ionics* 24:777–785
- Azlan AL, Isa MIN (2012) Proton conducting biopolymer electrolytes based on tapioca starch-NH₄NO₃. *Solid State Sci Technol Lett* 18:124–129
- Hucheng Z, Xiopeng X, Jianji W, Hanqing W (2003) FT-IR investigation of ion association in PEO-MSCN (M=Na, K) polymer electrolytes. *Solid State Ionics* 164:73–79
- Ramli MA, Chai MN, Isa MIN (2013) Influence of propylene carbonate as a plasticizer in CMC-OA based biopolymer electrolytes: conductivity and electrical study. *Adv Mater Res* 802:184–188
- Samsudin AS, Isa MIN (2012) Characterization of carboxy methylcellulose doped with DTAB as new types of biopolymer electrolytes. *Bull Mater Sci* 35:1123–1131
- Ahmad Z, Isa MIN (2012) Ionics conduction via correlated barrier hopping mechanisms in CMC-SA solid biopolymer electrolytes. *Int J Latest Res Sci Technol* 1:70–75
- Anji RP, Ranveer K (2011) Impedance spectroscopy and FTIR studies of PEG-based polymer electrolytes. *E-J Chem* 8:347–353
- Bhide A, Hariharan K (2007) Ionic transport studies on (PEO)₆:NaPO₃ polymer electrolyte plasticized with PEG400. *Eur Polym J* 43:4253–4270
- Woo HJ, Majid SR, Arof AK (2013) Effect of ethylene carbonate on proton conducting polymer electrolyte based on poly(ϵ -caprolactone) (PCL). *Solid State Ionics* 252:102–108
- Gupta S (2017) Varshney PK (2017) effect plasticizer concentration on structural and electrical properties of hydroxyethyl cellulose (HEC)-based polymer electrolyte. *Ionics* 23:1613–1617
- Kumar R, Sharma S, Pathak D, Dhiman N, Arora N (2017) Ionic conductivity, FTIR and thermal studies of nano-composite plasticized proton conducting polymer electrolytes. *Solid State Ionics* 305:57–62
- Jung SS, Kim KW, Ahn HJ, Ahn JH (2002) Preparation and characterization of plasticized polymer electrolytes based on the PVdF-HFP copolymer for lithium/sulfur battery. *J Mater Sci Mater Electron* 13:727–733
- Ahmad A, Isa KBM, Osman Z (2011) Conductivity and structural studies of plasticized polyacrylonitrile (PAN)—lithium triflate polymer electrolyte films. *Sains Malaysiana* 40:691–669
- Pradhan DK, Choudhary RNP, Samantaray BK (2008) Studies of dielectric relaxation and AC conductivity behavior of plasticized polymer nanocomposite electrolytes. *Int J Electrochem Sci* 3:597–608
- Samsudin AS, Isa MIN (2013) Conductivity and transport properties study of plasticized carboxymethyl cellulose (CMC) based solid biopolymer electrolytes (SBE). *Adv Mater Res* 856:118–122
- Buraidah MH, Arof AK (2011) Characterization of chitosan/PVA blended electrolyte doped NH₄I. *J Non-Cryst Solids* 357:3261–3266
- Rarmesh S, Leen KH, Kumutha K, Arof AK (2007) FTIR studies of PVC/PMMA blend based polymer electrolytes. *Spectrochim Acta A* 66:1237–1242
- Kim DW, Kim YR, Park JK, Moon SI (1998) Electrical properties of the plasticized polymer electrolytes based on acrylonitrile-methyl methacrylate copolymers. *Solid State Ionics* 106:329–337
- Zulkepli NAS, Tan W, Subban RHY (2017) Infrared studies of PVC-based electrolytes incorporated with lithium triflate and 1-butyl-3-methyl imidazolium trifluoromethanesulfonate as ionic liquid. *AIP Conf Proc* 10:1877–1844
- Chai MN, Isa MIN (2016) Novel proton conducting solid Biopolymer electrolytes based on Carboxymethyl cellulose doped with oleic acid and plasticized with glycerol. *Sci Rep* 6:27328–27334
- Abdul Rahaman H, Khandaker MU, Khan ZR, Kufian MZ, Noor IM, Arof AK (2014) Effect of gamma irradiation on poly(vinylidene difluoride)-lithium bis(oxalato) borate electrolyte. *Phys Chem Chem Phys* 16:11537–11157
- Arof AK, Amirudin S, Yusof SZ, Noor IM (2014) A method based on impedance spectroscopy to determine transport properties of polymer electrolytes. *Phys Chem Chem Phys* 16:1856–1867
- Sim LN, Arof AK (2017) Elastomers and their potential as matrices in polymer electrolytes. *INTECH* 10:5772–5809
- Muchakayala R, Song S, Gao S, Wang X, Fan Y (2017) Structure and ion transport in an ethylene carbonate-modified biodegradable gel polymer electrolyte. *Polym Test* 58:116–125
- Sownthari K, Suthanthiraraj SA (2014) Preparation and properties of a gel polymer electrolyte system based on poly ϵ -caprolactone containing 1-ethyl-3-methylimidazolium bis(trifluoromethylsulfonyl)imide. *J Phys Chem Solids* 75:746–751
- Aziz SB, Abdullah OG, Rasheed MA, Hameed HM (2017) Effect of high salt concentration (HSC) on structural, morphological, and electrical characteristics of chitosan based solid polymer electrolytes. *Polym* 9:187–206
- MacDonald JR (1987) Impedance spectroscopy emphasizing solid materials and systems. Wiley, Hoboken

36. Subba Reddy CV, Han X, Zhu QY, Mai LQ, Chen W (2006) Conductivity and discharge characteristics of (PVC + NaClO₄) polymer electrolyte systems. *Eur Polym J* 42:3114–3120
37. Selvasekarapandian S, Hema M, Kawamura J, Kamishima O, Baskaran R (2010) Characterization of PVA-NH₄NO₃ polymer electrolyte and its application in rechargeable proton battery. *J Phys Soc Jpn* 79SA:163–168
38. Subban RHY, Ahmad AH, Kamarulzaman N, Ali AMM (2005) Effects of plasticiser on the lithium ionic conductivity of polymer electrolyte PVC-LiCF₃SO₃. *Ionics* 11:442–445
39. Aziz SB, Kadir MFZ, Abidin ZHZ (2016) Structural, morphological and electrochemical impedance study of CS:LiTf based solid polymer electrolyte: reformulated Arrhenius equation for ion transport study. *Int J Electrochem Sci* 11:9228–9244
40. Che Balian SR, Ahmad A, Mohamed NS (2016) The effect of lithium iodide to the properties of carboxymethyl κ -carrageenan/carboxymethyl cellulose polymer electrolyte and dye-sensitized solar cell performance. *Polym* 8:163–173
41. Tiong TS, Buraidah MH, Teo LP, Arof AK (2016) Conductivity studies of poly(ethylene oxide)(PEO)/poly(vinyl alcohol) (PVA) blend gel polymer electrolytes for dye-sensitized solar cells. *Ionics* 22:2133–2142
42. Saxena A, Singh P, Bhattacharya B (2014) Structural and electrical studies of fullerene (C60) dispersed polymer electrolytes. *Mater Tehnol* 48:485–490
43. Shuhaimi NEA, Teo LP, Woo HJ, Majid SR, Arof AK (2012) Electrical double-layer capacitors with plasticized polymer electrolyte based on methyl cellulose. *Polym Bull* 69:807–826
44. Shukur MF, Itin R, Kadir MFZ (2014) Electrical properties of proton conducting solid biopolymer electrolytes based on starch-chitosan blend. *Ionics* 20:977–999
45. Bandara TMWJ, Mellander BE (2011) Evaluation of mobility, diffusion coefficient and density of charge carriers in ionic liquids and novel electrolytes based on a new model for dielectric response. *INTECH* 10:5772–15183
46. Samsudin AS, Isa MIN (2012) Structural and ionic transport study on CMC doped NH₄Br: a new types of biopolymer electrolytes. *J Appl Sci* 12:174–179
47. Kumar D, Hashmi SA (2010) Ion transport and ion-filler-polymer interaction in poly(methyl methacrylate)-based, sodium ion conducting, gel polymer electrolytes dispersed with silica nanoparticles. *J Power Sources* 195:5101–5108
48. Khair AS, Arof AK (2010) Conductivity studies of starch-based polymer electrolytes. *Ionics* 16:123–129
49. Kumar B, Scanlon LG, Spry RJ (2001) On the origin of conductivity enhancement in polymer-ceramic composite electrolytes. *J Power Sources* 96:337–342
50. Sharma JP, Sekhon SS (2005) Relative role of plasticizer and nano size fumed silica on the conductivity behaviour of PEO-NH₄PF₆ polymer electrolytes. *Ind J Eng Mater Sci* 12:557–562
51. Sharma S, Dhiman N, Pathak D, Kumar R (2016) Effect of nano-size fumed silica on ionic conductivity of PVdF-HFP-based plasticized nano-composite polymer electrolytes. *Ionics* 22:1865–1872
52. Samsudin AS, Isa MIN (2015) Conduction mechanism of enhanced CMC-NH₄Br biopolymer electrolytes. *Adv Mater Res* 1108:27–32
53. Buraidah MH, Teo LP, Majid SR, Arof AK (2009) Ionic conductivity by correlated barrier hopping in NH₄I doped chitosan solid electrolyte. *Phys B Condens Matter* 404:1373–1379
54. Rani MSA, Rudhzhiah S, Ahmad A, Mohamed NS (2014) Biopolymer electrolyte based on derivatives of cellulose from kenaf bast fiber. *Polym* 6:2371–2385
55. Starkey SR, Frech R (1997) Plasticizer interactions with polymer and salt in propylene carbonate-poly(acrylonitrile)-lithium triflate. *Electrochim Acta* 42:471–474
56. MacFarlane DR, Meakin P, Bishop A, McNaughton D, Rosalie JM, Forsyth M (1995) FTIR study of ion-pairing effects in plasticized polymer electrolyte. *Electrochim Acta* 40:2333–2337
57. Wang Z, Huang B, Huang H, Chen L, Xue R, Wang F (1996) Investigation of the position Li⁺ ions in a polyacrylonitrile based electrolyte by Raman and infrared spectroscopy. *Electrochim Acta* 41:1443–1446
58. Rasali NMJ, Samsudin AS (2017) Ionic transport properties of protonic conducting solid biopolymer electrolytes based on enhanced carboxymethyl cellulose-NH₄Br with glycerol. *Ionics* 10:1–12
59. Rozali MLH, Ahmad NH, Isa MIN (2015) Effect of adipic acid composition on structural and conductivity solid biopolymer electrolytes based on carboxy methylcellulose studies. *M Eurasian J Sustain Agric* 9:39–45
60. Rozali MLH, Ahmad Z, Isa MIN (2015) Interaction between carboxy methylcellulose and salicylic acid solid biopolymer electrolytes. *Adv Mater Res* 1107:223–229
61. Yu LH, Cheng WC, Chuh CY (2007) Conductivity and characterization of plasticized polymer electrolyte based on (polyacrylonitrile-b-polyethylene glycol) copolymer. *J Power Sources* 172:86–892
62. Samsudin AS, Aziz MIA, Isa MIN (2012) Natural polymer electrolyte system based on sago: structural and transport behavior characteristics. *Int J Polym Anal Charact* 17:600–607
63. Majid SR, Arof AK (2005) Proton-conducting polymer electrolyte films based on chitosan acetate complexed with NH₄NO₃ salt. *Phys B Condens Matter* 355:78–82
64. Gondaliya N, Kanchan DK, Sharma P (2013) Effect of a plasticizer on a solid polymer electrolyte. *Soc Plast Eng* 10:2417–2422
65. Chai MN, Isa MIN (2013) The oleic acid composition effect on the carboxymethyl cellulose based biopolymer electrolyte. *J Cryst Process Technol* 3:1–4
66. Kamarudin KH, Isa MIN (2013) Structural and DC ionic conductivity studies of carboxy methylcellulose doped with ammonium nitrate as solid polymer electrolytes. *Int J Phys Sci* 8:1581–1587
67. Majid SR, Arof AK (2007) Electrical behavior of proton-conducting chitosan-phosphoric acid-based electrolytes. *Physica B* 390:209–215
68. Woo HJ, Majid SR, Arof AK (2011) Conduction and thermal properties of a proton conducting polymer electrolyte based on poly (ϵ -caprolactone). *Solid State Ionics* 199:14–20
69. Ramli MA, Isa MIN (2016) Structural and ionic transport properties of protonic conducting solid biopolymer electrolytes based on carboxymethyl cellulose doped ammonium fluoride. *J Phys Chem B* 120:11567–11573
70. Ahmad NH, Isa MIN (2016) Characterization of un-plasticized and propylene carbonate plasticized carboxymethyl cellulose doped ammonium chloride solid biopolymer electrolytes. *Carbohydr Polym* 137:426–432
71. Fadzallah IA, Majid SR, Careem MA, Arof AK (2014) A study an ionic interactions in chitosan-oxalid acid polymer electrolyte membrane. *J Membr Sci* 463:65–72
72. Ahmad NH, Isa MIN (2015) Proton conducting solid polymer electrolytes based carboxymethyl cellulose doped ammonium chloride: ionic conductivity and transport properties. *Int J Plast Technol* 18:1–11
73. Samsudin AS, Kuan ECH, Isa MIN (2011) Investigation of the potential of proton-conducting biopolymer electrolytes based methyl cellulose-glycolic acid. *Int J Polym Anal Charact* 16:477–485
74. Okamoto Y, Yeh TF, Lee HS, Skotheim TA (1993) Design of alkaline metal ion conducting polymer electrolytes. *J Polym Sci A Polym Chem* 31:2573–2581
75. Rhoo HJ, Kim HT, Park JK, Hwang TS (1997) Ionic conduction in plasticized PVC/PMMA blend polymer electrolytes. *Electrochim Acta* 42:1571–1579

76. Samsudin AS, Khairul WM, Isa MIN (2012) Characterization on the potential of carboxy methylcellulose for application as proton conducting biopolymer electrolytes. *J Non-Cryst Solids* 358:1104–1112
77. Itoh T, Miyamura Y, Ichikawa Y, Uno T, Kubo M, Yamamoto O (2003) Composite polymer electrolytes of poly(ethylene oxide)/BaTiO/Li salt with hyperbranched polymer. *J Power Sources* 119:403–408
78. Rajendran S, Babu RS, Sivakumar P (2008) Investigations on PVC/PAN composite polymer electrolytes. *J Membr Sci* 315:67–73
79. Leo CJ, Subba Rao GV, Chowdari BVR (2002) Studies on plasticized PEO–lithium triflate–ceramic filler composite electrolyte system. *Solid State Ionics* 148:159–171
80. Ahmad NH, Isa MIN (2015) Structural and ionic conductivity studies of CMC based polymer electrolyte doped with NH₄Cl. *Adv Mater Res* 1107:247–252
81. Chowdhury FI, Khandaker MU, Amin YM, Kufian FZ, Woo HJ (2017) Vibrational, electrical, and structural properties of PVDF-LiBOB solid polymer electrolyte with high electrochemical potential window. *Ionics* 23:275–284
82. Ibrahim S, Mohd Yasin SM, Nee NM, Ahmad R, Johan MR (2012) Conductivity, thermal and infrared studies on plasticized polymer electrolytes with carbon nanotubes as filler. *J Non-Cryst Solids* 358:210–216
83. Rahaman MHA, Khandaker MU, Khan ZR, Kufian MZ, Noor ISM, Arof AK (2014) Effect of gamma irradiation in poly(vinylidene difluoride)-lithium Bis(oxalate)borate electrolytes. *Phys Chem Chem Phys* 16:11527–11537
84. Zhou XY, Cui YF, Jia DM, Xie D (2009) Effect of a complex plasticizer on the structure and properties of the thermoplastic PVA/starch blends. *J Polym-Plast Technol Eng* 48:489–495